Eduardo V. Liberado[1], Wesley A. Souza[1], José A. Pomilio[1], Helmo K. M. Paredes[2], Fernando P. Marafão[2]

UNICAMP - University of Campinas (1), UNESP - Univ Estadual Paulista (2)

Design of Static var Compensators using a General Reactive Energy Definition

***Abstract**. This paper describes a methodology to design Static var Compensators (SVC) using the reactive energy definition from the Conservative Power Theory. The application of this methodology is presented through simulations of local and distributed compensation scenarios. Results show effective compensation of reactive current and load unbalance. Moreover, the harmonic distortion caused by thyristor controlled reactor has been suitable attenuated by passive filters designed in combination with the SVC.*

***Streszczenie.** Opisano metodologię projektowania kompensatora mocy biernej SVC wykorzystującą definicję energii biernej z Teorii Konserwacji Mocy. Symulacje wykazały że układ kompensuje prąd bierny i nierówność obciążenia. Tłumione są także harmoniczne. (**Projektowanie kompensatora mocy biernej na podstawie definicji energii biernej**)*

Keywords: Arc Furnace, Conservative Power Theory, Reactive Compensation, Static var Compensator, Unbalance Compensation.
Słowa kluczowe: kompensator mocy biernej, teoria konserwacji mocy.

Introduction

Power conditioning plays an important role in recent researches related to smart grids [1]. Different approaches have been proposed to control compensators that are distributed along the network, in order to reach a cooperative operation, the sharing of compensation demands and the avoidance of detrimental interaction among distinct compensation architectures [2-8].

However, these approaches are mainly focused on the use of inverter-based compensators [2-4,7], while traditional passive technologies still may contribute to grid optimization in the smart grid context, as initially proposed in [5,6], when different architectures of compensators were used and controlled cooperatively. Nevertheless, the design and control of traditional compensators should be reviewed and adapted.

Thus, this paper presents a designing methodology for Static var Compensators (SVC) based on the reactive energy definition from the Conservative Power Theory (CPT) [8], which is a conservative term and remains valid under unbalanced, nonsinusoidal or variable frequency conditions. The goals of the designed SVC are reactive and load imbalance compensation, and due to the use of conservative quantities in its control, it may be applied to cooperative compensation approaches for smart grids.

Conservative Power Theory - Background

The Conservative Power Theory (CPT) is a recent mathematical formulation that associates characteristics of electrical circuits to current and power components [8]. Their definitions have been applied to design and control of compensators [6,7,9,10], as well as to accountability and revenue metering proposals [11]. In this paper, CPT will be briefly presented, and additional details of these definitions can be found in [8].

A. Conservative quantities

The two conservative quantities defined by CPT are instantaneous active power *p(t)* and instantaneous reactive energy *w(t)*. For a M-phase circuit on which the voltages *u(t)* and currents *i(t)* respect the Kirchhoff laws, that quantities for each phase may be expressed by:

(1.a) $$p_m(t) = u_m(t).i_m(t),\ \ m = 1 \dots M$$

(1.b) $$w_m(t) = \hat{u}_m(t).i_m(t), m = 1 \dots M$$

such that û is the unbiased voltage integrals, i. e., the time integral of voltage minus the average value of such integral function. If the sum of the values of p_m (or w_m) from all phases results zero at every instant, this quantity is conservative for any waveform of voltages and currents [8]. The same conclusions arise if one considers different nodes in a particular power grid.

The average values of (1.a) and (1.b) results in active power and reactive energy for each phase, as expressed by (2.a) and (2.b). It is important to mention that reactive energy may result in positive or negative values, depending if load has an inductive or capacitive characteristic.

(2.a) $$P_m = \frac{1}{T}\int_0^T p_m(t)dt,\ \ m = 1 \dots M$$

(2.b) $$W_m = \frac{1}{T}\int_0^T w_m(t)dt, m = 1 \dots M$$

B. Current and power decomposition

According to CPT, the electrical current of a polyphase system may be decomposed into five orthogonal components and each of them represents a specific characteristic of the electrical circuits. Furthermore, each current component is associated to a power component, and they may be described as follows.

Active balanced current (i_a^b): it is the minimum current responsible for transfer active power to the load. The product of collective values[1] of voltages and active balanced currents is the active power ($P = \boldsymbol{U}\boldsymbol{I}_a^b$), which results in the same value if calculated by the sum of the P_m defined in (2.a) from the *M*-phases of that circuit. This definition of active power matches with the traditional definitions of active power [12].

Reactive balanced current (i_r^b): represents the stored energy in the circuit (phase displacement between voltage and current). This component is associated to reactive power Q by the product of collective values ($Q = \boldsymbol{U}\boldsymbol{I}_r^b$). The reactive power may be associated to reactive energy only in a determined frequency.

Active unbalanced current (i_a^u): this current component appears due to unbalanced equivalent conductances in the phases of the circuit.

Reactive unbalanced current (i_r^u): this current component appears due to unbalanced equivalent reactivities in the phases of the circuit.

The unbalance current components can be associated to a unique unbalance power component N that quantifies the effect of unbalanced loads connected to the network. Thus, the unbalance power may be obtained by $\left(N = \boldsymbol{U}\sqrt{\boldsymbol{I}_a^{u\,2} + \boldsymbol{I}_r^{u\,2}}\right)$.

[1] The collective value of voltages or currents from a three-phase circuit is defined as: $\boldsymbol{X} = \sqrt{X_a^2 + X_b^2 + X_c^2}$, where X_a, X_b, X_c are RMS values of the three phases.

Void current (i_v): reflects the non linearity between voltage and current, which are caused mainly by electronic loads. This current component does not transfer active power or reactive energy through the network, and a particular power component is associated to it, the distortion (or void) power ($D = \boldsymbol{U}\boldsymbol{I}_v$).

The total power in a determined point of the circuit, e. g. the Point of Common Coupling (PCC), is the apparent power A, and it is calculated by the product between the collective values of voltage and the total current at PCC ($A = \boldsymbol{U}\boldsymbol{I}$).

C. Power factor

The power factor (λ) defined by CPT is the ratio between the active power and the apparent power, as shown in (3).

(3) $$\lambda = \frac{P}{A} = \frac{\boldsymbol{I}_a^b}{\boldsymbol{I}}$$

Although (3) is similar to the conventional definition of power factor, λ remain valid even under non-ideal voltage conditions, because it is not related to fasorial characteristics and it is unity only in case of pure balanced resistive load. Thus, this definition of power factor may represent a global efficiency factor.

Static var Compensators

A. Design of SVC components

The proposed architecture of SVC is represented in Fig.1. It is a three phase delta connected compensator composed by thyristor switched capacitors (TSC) and thyristor controlled reactors (TCR).

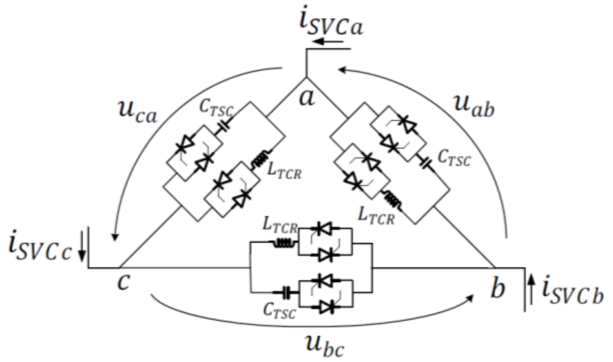

Fig. 1. Architecture of the SVC.

All the variables used in the design of SVC are measured or calculated considering the voltages and currents at the point that is the goal of compensation, i. e., the PCC of the network.

The SVC goal is to compensate both reactive and unbalance currents defined by CPT. Thus, the design of the SVC may consider two conditions: if the currents at PCC are balanced but contain balanced reactive currents, only TSC is used. Thus, $i_{SVCm} = i_{rm}^b,\ \ m = a, b, c$; and the minimum capacitance to compensate i_{SVCm} is obtained by (4), in which U_L is the RMS value of line voltages at PCC and ω is the fundamental angular frequency.

(4) $$C_{TSC} = \frac{I_{SVCm}}{\omega U_L\sqrt{3}} = \frac{I_{rm}^b}{\omega U_L\sqrt{3}}$$

Another condition is: in the presence of balanced reactive current and unbalance currents at PCC, both TSC and TCR are used, and ever since the currents are different in each phase due to the load unbalance, the maximum value of i_{SVCm} must be considered, i. e., $i_{SVCm\acute{a}x} = max\left(\{i_{rm}^b + i_{am}^u + i_{rm}^u\}_{m=a,b,c}\right)$. In this case, TSC should compensate not only the reactive current from the load, but also the balanced reactive current from TCR. Considering that the current drained by TCR equals to $i_{SVCm\acute{a}x}$, the relation between TCR and TSC reactances at fundamental frequency is expressed by:

(5) $$X_{TSC} = 2X_{TCR}$$

Thereby, the capacitance of TSC and inductance of TCR may be obtained from (5):

(6) $$C_{TSC} = \frac{I_{SVCm\acute{a}x}}{\omega U_L\sqrt{3}};\ L_{TCR} = \frac{U_L\sqrt{3}}{2\omega\ I_{SVCm\acute{a}x}}$$

One may observe that the term ω would limit the compensation only to fundamental frequency, but the efficiency is not severely reduced if the SVC is designed considering the RMS values obtained from measured voltages and currents under unbalanced and/or distorted conditions, and due to orthogonality among the current components, it is possible to extract the correct value of each component to be compensated in any condition.

B. SVC operation

The TSC banks must be switched only in the zero crossing of line voltages, while the thyristors of the TCR must be fired with an angle α in every cycle of the line voltages. The angle α may be determined by the equivalent average reactive energy that would flow through the SVC, which is expressed in (7):

(7) $$\begin{aligned} W_{ab} &= -W_{ab}^{\alpha} + W_{TSC} \\ W_{bc} &= -W_{bc}^{\alpha} + W_{TSC} \\ W_{ca} &= -W_{ca}^{\alpha} + W_{TSC} \end{aligned}$$

such that:

W_{ab}, W_{bc} e W_{ca} are the equivalent reactive energies of each branch of the SVC;

W_{ab}^{α}, W_{bc}^{α} e W_{ca}^{α} are the equivalent reactive energies of each TCR, when it is switched with a conduction angle α in relation to line voltages. They may be calculated by the average reactive energies of the three phases at PCC:

(8) $$\begin{aligned} W_{ab}^{\alpha} &= W_a + W_b - W_c \\ W_{bc}^{\alpha} &= -W_a + W_b + W_c \\ W_{ca}^{\alpha} &= W_a - W_b + W_c \end{aligned}$$

W_{TSC} is the reactive energy of each branch of TSC, calculated by $C_{TSC}.U_L^2$.

Therefore, the conduction angle of each TCR is determined by solving equations (9), in which W_{TCR} is the total reactive energy of each TCR, calculated by $\widehat{U}_L^2/L_{TCR}$.

(9) $$\begin{aligned} W_{ab} &= \frac{W_{TCR}}{\pi}(2\pi - 2\alpha_{ab} + sin\,2\alpha_{ab}) \\ W_{bc} &= \frac{W_{TCR}}{\pi}(2\pi - 2\alpha_{bc} + \sin 2\alpha_{bc}) \\ W_{ca} &= \frac{W_{TCR}}{\pi}(2\pi - 2\alpha_{ca} + \sin 2\alpha_{ca}) \end{aligned}$$

C. Design of passive filters

The switching of TCR causes harmonic distortion in the currents, which has been mitigated by passive filters (PF) tuned at 5th, 7th, 11th and, due to the switching of unbalanced reactors, 3rd harmonic frequencies [13].

Considering that the capacitances of passive filters may over-compensate the reactive current at low frequencies, the additional reactive energy due to these capacitors should be considered in W_{TSC}, which can be re-written as:

(10) $$W_{TSC} = (C_{TSC} + C_{PF}).U_L^2$$

such that C_{PF} is the capacitance of the passive filter.

Consequently, (9) would result in proper angles to avoid reactive over-compensation.

It is important to observe that the additional reactive energy from PF capacitors plus W_{TSC} should not exceed W_{TCR}, in order to maintain the angles α into the interval [π/2, π] rad.

After determining C_{PF} in relation to TCR, it is converted to wye and divided by the number of harmonic components to be attenuated by PF. Thus, the inductors are tuned into each harmonic component and the corresponding resistances are determined by (11):

(11) $R_h = \frac{2\pi f_h L_h}{MF}$

such that:

R_h, L_h are the resistance and tuned inductance at each harmonic frequency f_h;

MF is the merit factor, used to reduce filter selectivity. Its typical values vary from 40 to 200 [5].

D. SVC control strategy

The proposed control strategy to adjust the SVC components in case of load variation is presented in Fig. 2. Essentially, when the average value of load reactive energy varies, C_{TSC} is re-calculated. Due to the limited number of capacitor banks installed, if C_{TSC} does not match the available TSC, only TCR conduction angles will be updated. Otherwise, W_{TSC} is re-calculated according to (10), TSC is switched in the next zero-crossing of each line voltage and the conduction angles are calculated to compensate the change in the load and in TSC. It is important to mention that for a variable load case, the capacitance of the passive filters should be determined considering the maximum value of W_{TSC}, which corresponds to the worst case.

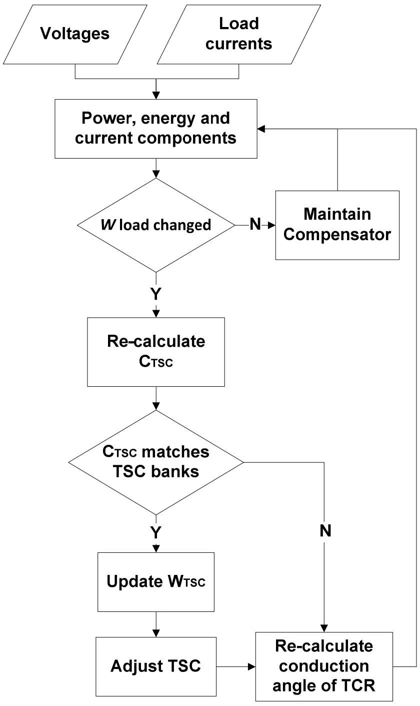

Fig. 2. Control strategy for SVC in case of load variation.

Simulation Results

A. Local compensation of an electric arc furnace

In this application, the SVC is used to increase power factor at the PCC, by compensating the variable reactive and unbalance power components. The electric arc furnace (EAF) model simulated on PSCAD is based on [14,15]. It consists on a variable resistance that is a function of the electrical arc length in every phase of the melting process. Fig.3 represents the topology of the compensators in the simulated circuit. The PCC is located at medium voltage side and the reference for voltages is a virtual star point, as recommended in [8].

Thus, the electric arc length is configured to simulate three stages of loading and melting and the stage of refining at the end of the process [16]. The lengths are different in each phase of the system in order to produce load unbalance. The simulation total time was 11.6 s, which in real furnaces would correspond to at least 80 minutes. Fig.4 presents the CPT power components, power factor and reactive energies at PCC without compensation.

All power components are oscillating during the four stages of arc furnace. Apparent power reaches 69.0 MVA during the loading and refining stages, while unbalance power is equal to 2.8 MVA and distortion power is 2.5 MVA. Power factor oscillates from 0.6276 to 0.2386. The reactive energies is unbalanced due to the different values of arc length in each phase. Total Harmonic Distortion (THD) in the PCC currents oscillates between 1.0% and 4.9%, while voltage's THD varies between 0.6% and 1.7%.

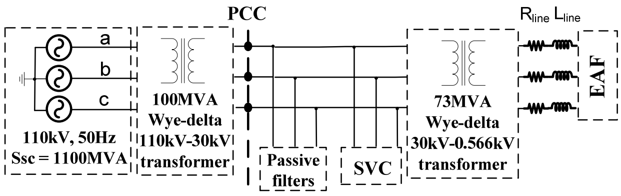

Fig. 3. Topology of the compensators for local compensation. Equivalent line impedance: R_{line} = 0,478mΩ; L_{line} = 10,66μH.

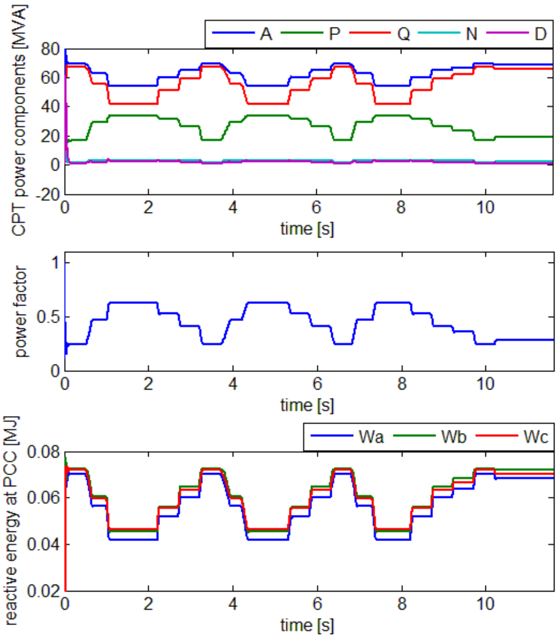

Fig. 4. CPT power components, power factor and reactive energies at PCC without compensators.

Table 1 presents the designed components of the SVC and PF (passive filter). TSC banks were designed to result in a proper capacitance value for each steady state level of power components from Fig. 4. The additional reactive energy of PF capacitors is 15% of W_{TSC} in the worst case, when the reactive energies from the load are in their maximum values. The merit factor adopted was 200.

Table 1. Designed parameters for the SVC and the passive filter.

L_{TCR} = 36.6mH	
TSC values	
163.6 μF (worst case); 154.8 μF; 146.7μF;137.5 μF;126.2 μF;103.9 μF	
Capacitor in each PF branch = 36.7μF	
R_3 = 173 mΩ; R_5 = 103.8 mΩ	L_3 = 36.7 mH; L_5 = 13.2 mH
R_7 = 74.0 mΩ; R_{11} = 47.0 mΩ	L_7 = 6.7 mH; L_{11} = 2.7 mH

Fig.5 presents the CPT power components, power factor and reactive energies at PCC when the compensators are operating. The flow of reactive energies at PCC is closed to zero during all the simulation. Consequently, reactive power and apparent power are reduced too. Unbalance power is limited between 0.926 MVA and 0.578 MVA and distortion power is 2.2 MVA, which indicates that most part of harmonic distortion caused by the load is not mitigated, but the main harmonic components caused by TCR are reduced and do not have a big contribution to the PCC harmonic distortion. The power factor varies between 0.9834 and 0.9538.

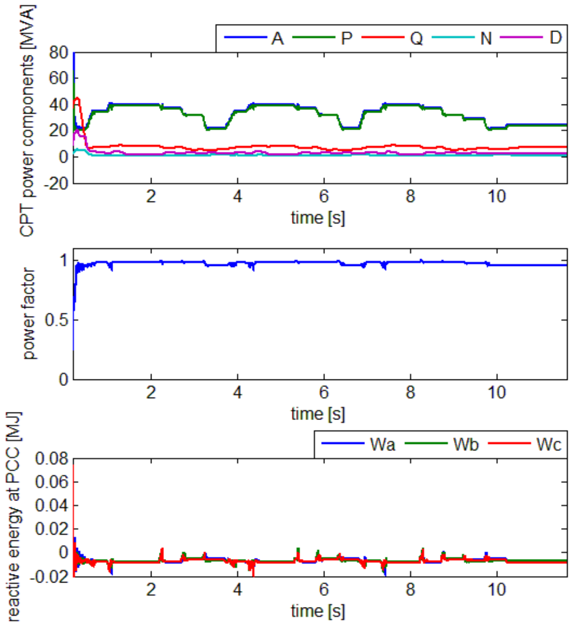

Fig. 5. CPT power components, power factor and reactive energies at PCC without compensators.

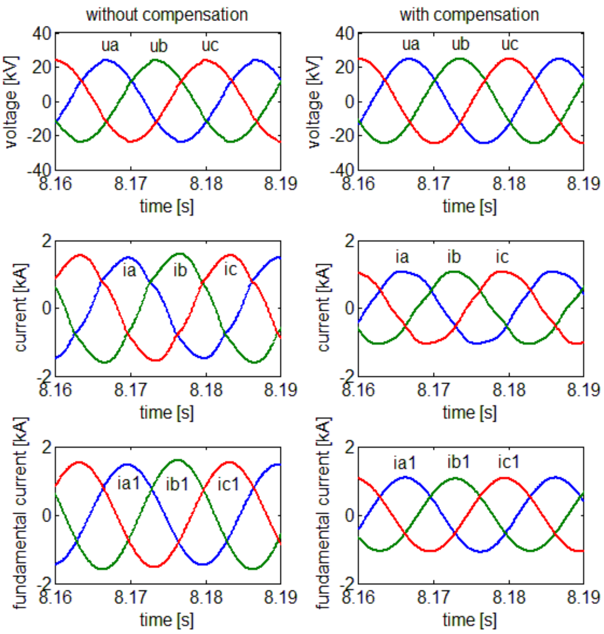

Fig. 6. Voltages (top), total currents (center) and fundamental component of the currents (bottom) at PCC with (left) and without (right) compensation.

Fig.6 shows the waveforms of the voltages, currents and the fundamental currents measured at PCC with and without compensation. During the period shown in Fig.6, the EAF is in the melting stage with the maximum apparent power, and the compensation of load unbalance and reactive power is effective (even if the total currents are distorted, the fundamental currents are balanced and almost in phase with the voltages). The power factor is 0.9792, the current's THD is 4.0% and the voltage's THD is 0.75%. However, current's THD oscillates between 10.5% and 3.5% during this simulation, because the fundamental components are more reduced by compensation than the harmonic components. The voltage's THD is limited between 1.2% and 0.7%.

Fig.7 presents the variation of TSC and conduction angles of TCR during the compensation. One may observe that TSC follows the reactive energy of the load, while TCR compensate it with an opposite behavior.

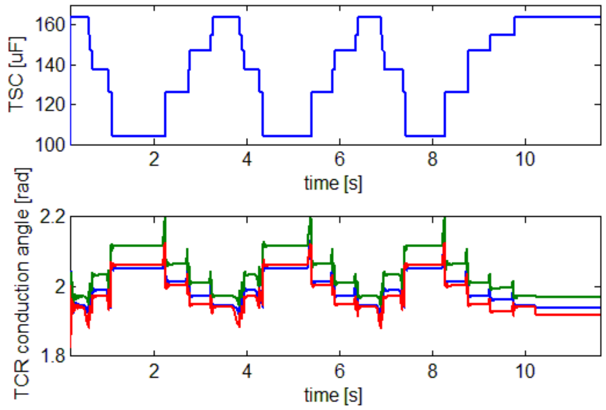

Fig. 7. TSC values (top) and TCR conduction angles (bottom).

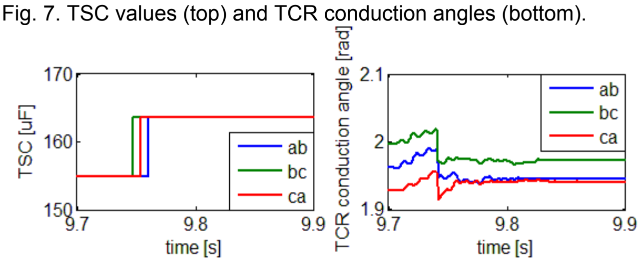

Fig. 8. Highlighted interval from each graphic from Fig. 7.

Moreover, Fig. 8 presents a highlighted interval from the graphics of Fig. 7, showing the time response of SVC variables: conduction angles of TCR follows the load variation at any instant, while TSC follows the load variation according to the number of possible capacitance values and within one cycle of each line voltages.

Distributed compensation results

In order to evaluate the effectiveness of the proposed methodology in a distributed compensation approach, a distribution network based on IEEE 13 node distribution test feeder [17] was simulated. Fig.9 represents this network with the number of conductors in each branch.

Node 650 is feed by an 115 kV source. The delta-grounded wye 5 MVA substation transformer between nodes 650 and 632 reduces the voltage level to 4.16 kV, and the grounded wye-grounded wye 500 kVA transformer between nodes 633 and 634 reduces the voltage level from 4.16 kV to 480 V.

Transmission lines were modeled using impedance and capacitance matrices. Loads are RL connected in delta or between two phases, so there is no return conductor on this network. Additionally, a single phase 100 kvar capacitor bank was connected to phase c of node 611 and a three-phase 600 kvar capacitor bank was connected to node 675.

Node 632 was adopted as the PCC of this network, so the compensation goals and the design of the compensators were related to this node. The waveforms of voltages and currents were measured at nodes 632 and 671, in order to evaluate the effects of compensation not only at PCC, but also at other points of the network.

The simulation of this 13 node network without compensators results in the values shown in Table 2. Fig. 10 shows voltage and current waveforms at nodes 632 and 671.

To compensate reactive and unbalance power at PCC, two SVCs were designed, one considering 70% of I_{SVCmax}

measured at node 632 and other considering 30% of that current. For the passive filters, the maximum additional reactive energy that may be compensated by TCRs was 25% of W_{TSC}.

Table 3 presents the values of the two designed compensation units, the one with 70% of compensation demand was connected to node 633 and the other was connected to node 680.

Since the conduction angle α_{bc} results close to π/2rad, one may observe that the range of additional reactive energy adopted, which may be compensated by TCR, is the maximum in this application.

The simulation total time was 1.6 s and the compensators were turned on at t = 0.5 s. Table 4 shows the voltage, current, power, power factor and total harmonic distortion (THD) of voltages and currents at node 632 after compensation.

The power factor was close to unity and both reactive and unbalance power were considerably reduced at PCC. Moreover, distortion power and harmonic distortion were maintained under suitable values by the passive filters.

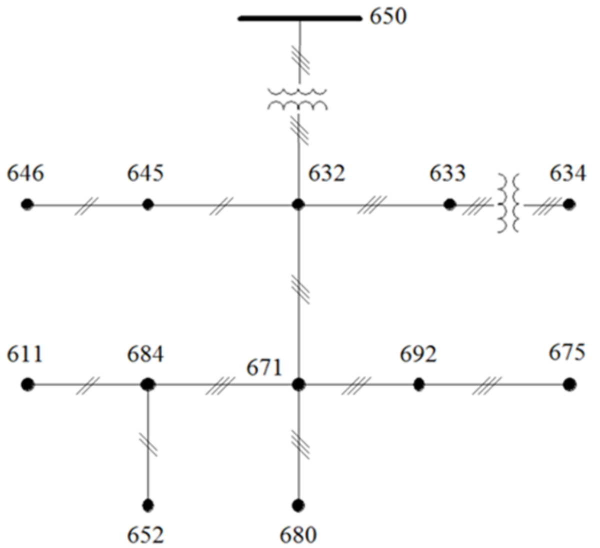

Fig. 9. IEEE 13 node test feeder-based network [17].

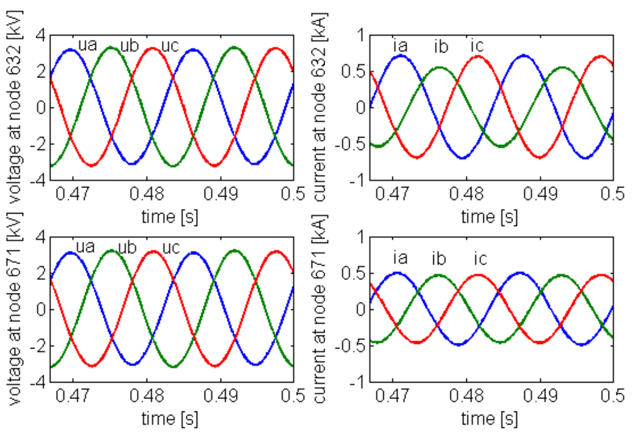

Fig. 10. Voltages (left) and currents (right) at PCC (node 632) and node 671 without compensation.

Fig.11 presents the waveforms of the voltages, currents and its fundamental component at node 632 and currents at node 671 after compensation. Both voltages and currents from node 632 were balanced and may be considered sinusoidal, while currents from node 671 were not so much affected by the compensation.

The results of this simulation show that compensation demand from a determined node may be effectively shared among compensators with different capacities and distributed along the network.

Table 2. Voltage, current, power, energy and power factor values at node 632 (PCC) without compensation.

U_a = 2.235 kV	U_b = 2.303 kV		U_c = 2.283 kV	
I_a = 0.500 kA	I_b = 0.387 kA		I_c = 0.493 kA	
W_a = 1.536 kJ	W_b = 1.011 kJ		W_c = 0.808 kJ	
A [MVA]	P [MW]	Q [Mvar]	N [MVA]	D [MVA]
3.156	2.843	1.265	0.527	0
λ = 0.9007				

Table 3. Designed parameters of the two SVC and passive filters.

SVC at node 633	SVC at node 680
C_{TSC}= 120.5μF; W_{TSC}= 1.931 kJ	C_{TSC}= 51.64μF; W_{TSC}=0.827kJ
L_{TCR} = 50.6mH; W_{TCR}=2.223 kJ	L_{TCR} = 118mH; W_{TCR}=0.955kJ
W_{ab}= 1.196 kJ; W_{bc}= 2.216 kJ W_{ca}= 1.481 kJ	W_{ab}= 0.513 kJ; W_{bc}= 0.950 kJ W_{ca}= 0.635 kJ
α_{ab}= 1.956 rad; α_{bc}= 1.579 rad α_{ca}= 1.844 rad	α_{ab}= 1.962 rad; α_{bc}=1.583rad α_{ca}= 1.849 rad
Capacitance of each PF branch: 22.6 μF	Capacitance of each PF branch: 9.7 μF
R_3 = 196 mΩ; R_5 = 117 mΩ	R_3 = 457 mΩ; R_5 = 274 mΩ
R_7 = 84 mΩ; R_{11} = 53 mΩ	R_7 = 196 mΩ; R_{11} = 125 mΩ
L_3 = 35 mH; L_5 = 12.5 mH	L_3 = 81 mH; L_5 = 29 mH
L_7 = 6 mH; L_{11} = 2 mH	L_7 = 15 mH; L_{11} = 6 mH

Table 4. PCC variables with compensation.

U_a = 2.348 kV	U_b = 2.374 kV		U_c = 2.352 kV	
I_a = 0.435 kA	I_b = 0.435 kA		I_c = 0.446 kA	
W_a = 0.108 kJ	W_b = 0.000 kJ		W_c = 0.003 kJ	
THDia = 0.784%	THDib = 1.909%		THDic = 1.387%	
THDua = 0.341%	THDub = 0.560%		THDuc = 0.454%	
A [MVA]	P [MW]	Q [Mvar]	N [MVA]	D [MVA]
3.104	3.102	0.053	0.067	0.047
λ = 0.9995				

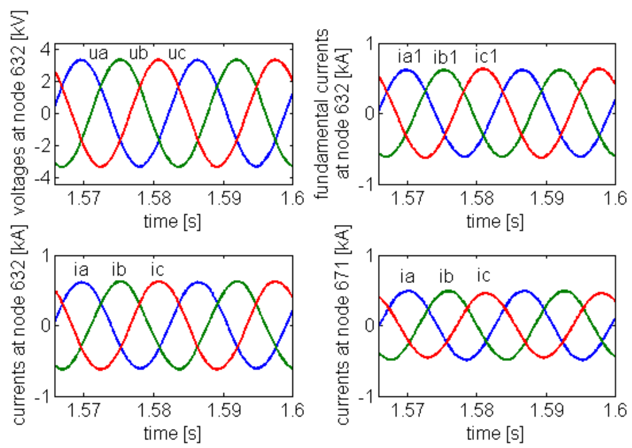

Fig. 11. Voltages (top left) and currents (bottom left) at PCC (node 632), fundamental currents (top right) from PCC and currents from node 671 (bottom right) after compensation.

Another interesting result is that the instantaneous reactive energy at node 632 remained conservative during all the simulation, which can be observed in Fig.12 that presents the sum of the instantaneous reactive energies from the three phases of node 632 at each instant. As it always results zero, the instantaneous reactive energy is conservative and may be used to control distributed compensators in case of variable loads.

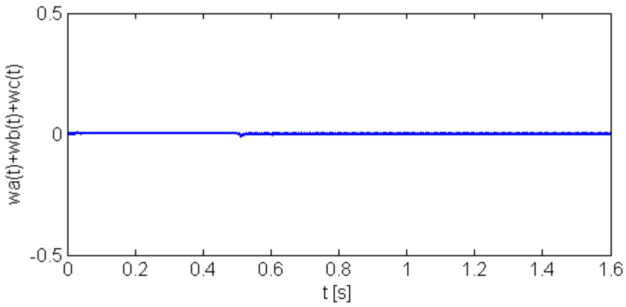

Fig. 12. Sum of instantaneous reactive energies from node 632 at each instant of simulation.

Conclusion

This paper presented a new methodology to design SVC and its passive filters by using the recently defined reactive energy concept.

The results show suitable compensation of reactive and unbalance current considering an electrical arc furnace (EAF) as a load. The harmonic distortion caused by TCR was also mitigated and the power factor ended close to unity.

The application of such methodology in distributed compensation was also effective, and the reactive energy from PCC was shared between two compensation units connected to different points in the grid.

The simulations presented here, likewise the discussions in [5,6], indicate that reactive energy may be a fundamental variable to insert traditional passive and/or quasi-stationary compensation technologies in the modern power system scenario.

The authors wish to express their gratitude to FAPESP (São Paulo Research Foundation, Process 2013/08545-6), CNPq (Process 133678/2010-5) and Capes for supporting this research.

REFERENCES

[1] R. Strzelecki and G. Benysek, "*Power Electronics in Smart Electrical Energy Networks*", 1st Ed., Springer, Poland, 2008.

[2] P. Jintakosonwit, H. Fujita, H. Akagi, and S. Ogasawara, "Implementation and Performance of Cooperative Control of Shunt Active Filters for Harmonic Damping Throughout a Power Distribution System," *IEEE Transactions on Industry Applications*, vol. 39, no. 2, 2003, pp. 556-564.

[3] P. T. Cheng, T. L. Lee, H. Akagi and H. Fujita, "A Dynamic Tuning Method for Distributed Active Filter Systems," *IEEE IAS 41th Annual Meeting*, 2008, pp. 175 - 182.

[4] P. T. Cheng and C. Chen, "A Cooperative Imbalance Compensation Method for Distributed-Generation Interface Converters," *IEEE Transactions on Industry Applications*, vol. 45, no. 2, 2009, pp. 805-815.

[5] E. Tedeschi and P. Tenti, "Cooperative Design and Control of Distributed Harmonic and Reactive Compensators," *Przeglad Elektrotechniczny*, vol. 84, no 6, 2008, pp. 23-27.

[6] H. K. M. Paredes, A. Costabeber, and P. Tenti, "Application of Conservative Power Theory to Cooperative Control of Distributed Compensators in Smart Grids," *Przeglad Elektrotechniczny*, vol. 87, 2011, pp. 1-7.

[7] P. Tenti, A. Costabeber, and P. Mattavelli, "Improving power quality and distribution efficiency in micro-grids by cooperative control of Switching Power Interfaces," *IEEJ Transactions on Industry Applications*, vol. 131, no. 12, 2011, pp. 1364-1372.

[8] P. Tenti, P. Mattavelli, and H. K. M. Paredes, "Conservative Power Theory, Sequence Components and Accountability in Smart Grids," *Przeglad Elektrotechniczny*, vol. 86, no 6, 2010, pp. 30-37.

[9] H. K. M. Paredes, L. C. P. Silva, D. I. Brandão, F. P. Marafão, "Possible Shunt Compensation Strategies Based on Conservative Power Theory", *Przeglad Elektrotechniczny*, vol. 87, no. 1, 2011, pp. 34-39.

[10] F. M. Marafão, D. I. Brandão, F. A. S. Gonçalves and H. K. M. Paredes, "Decoupled reference generator for shunt active filters using the conservative power theory," Journal of Control, Automation and Electrical Systems, vol. 24, no. 4, pp. 522-534, 2013.

[11] H. K. M. Paredes, F. P. Marafão, P. Mattavelli, P. Tenti, "Application of Conservative Power Theory to Load and Line Characterization and Revenue Metering", *Proc. of International Workshop on Applied Measurements for Power Systems*, Achen, 2012.

[12] F. P. Marafão, E. V. Liberado, H. K. M. Paredes and L. C. P. Silva, "Three-phase four-wire circuits interpretation by means of different power theories," *Przeglad Elektrotechniczny*, vol. 87, no. 1, 2011, pp. 28-33.

[13] San-Yi Lee and Chi-Jui Wu, "Combined compensation structure of an SVC and an active filter for unbalanced three phase distribution feeders with harmonic distortion," *Proc. of APSCOM-97. Fourth International Conference on Advances in Power System Control, Operation and Management*, Hong Kong, 1997, pp. 543-548.

[14] M. Panoiu, C. Panoiu, I. Sora, M. Osaci, "About the Possibility of Power Controlling in the Three-Phase Electric Arc Furnaces Using PSCAD EMTDC Simulation Program", *Advances in Electrical and Computer Engineering*, vol. 7, no. 1, 2007, pp; 38-43.

[15] M. Panoiu, C. Panoiu, I. Sora, A. Iordan, "Study about the Process Control of an Electric Arc Furnace using Simulations based on an Adaptive Algorithm", *WSEAS Transactions on Information Science and Applications*, vol. 5, 2008, pp. 1628-1637.

[16] M. R. Candido, L. C. Zanetta, "A Wavelet-Based Algorithm for Power Quality detection in Electric Arc Furnace", *Proc. of Transmission and Distribution Conference and Exposition*, IEEE/PES, 2008, pp. 1-6.

[17] IEEE Power & Energy Society. "Distribution Test Feeders". http://ewh.ieee.org/soc/pes/dsacom/testfeeders/index.html.

***Authors**: Eduardo Verri Liberado, University of Campinas (UNICAMP), School of Electrical and Computer Engineering (FEEC), Department of Energy Control and Systems (DSCE), Av. Albert Einstein 400, 13083-852, Campinas – SP – Brazil, E-mail: eduardo.verri.liberado@gmail.com.*

Wesley Angelino de Souza, University of Campinas (UNICAMP), School of Electrical and Computer Engineering (FEEC), Department of Systems of Electrical Energy (DSEE), Av. Albert Einstein 400, 13083-852, Campinas – SP – Brazil, E-mail: wesley@fc.unesp.br.

José Antenor Pomílio, University of Campinas (UNICAMP), School of Electrical and Computer Engineering (FEEC), Av. Albert Einstein 400, 13083-852, Campinas – SP – Brazil, E-mail: antenor@fee.unicamp.br.

Helmo Kelis Morales Paredes, Univ Estadual Paulista (UNESP), Campus of Sorocaba, Group of Automation and Integrated Systems, (GASI), Av. Três de Março 511, 18087-180, Sorocaba – SP – Brazil, E-mail: hmorales@sorocaba.unesp.br.

Fernando Pinhabel Marafão, Univ Estadual Paulista (UNESP), Campus of Sorocaba, Group of Automation and Integrated Systems, (GASI), Av. Três de Março 511, 18087-180, Sorocaba – SP – Brazil, E-mail: fmarafao@sorocaba.unesp.br.